

## GALACTIC SUPERWIND: COLD VERSUS HOT MODEL

S. A. Silich

Instituto Nacional de Astrofísica Óptica y Electrónica, Puebla, México

### RESUMEN

Reanalizo la solución de viento supergaláctico en estado estacionario que es bien conocida. Muestro que los supervientos impulsados por los brotes compactos y poderosos de estrellas sufren un enfriamiento catastrófico cerca de la superficie del cúmulo estelar y establecen distribuciones de temperatura que son radicalmente diferentes a la solución adiabática. Se discuten las implicaciones observacionales del modelo de viento frío tanto en rayos-X como en el régimen de líneas ópticas.

### ABSTRACT

Here I reanalyze the well-known steady-state supergalactic wind solution. I show that superwinds driven by compact and powerful starbursts undergo a catastrophic cooling close to the star cluster surface and establish temperature distributions that are radically different from the adiabatic solution. The observational implications of the cold wind model both in X-ray and visible line regimes are discussed.

*Key Words:* **GALAXIES: ISM — GALAXIES: STARBURST — HYDRODYNAMICS**

### 1. INTRODUCTION

Star-formation activity approaches its maximum level in starburst galaxies. Starbursts are found both at high and intermediate redshifts (Dawson et al. 2002; Pettini et al. 1998) as well as in the local universe (Marlowe et al. 1995; Cairos et al. 2001). Energy deposition by stellar winds and SNe explosions within star-forming regions generates strong shock waves which collect interstellar gas and create superbubbles, with characteristic sizes ranging from several hundred parsecs to a few kiloparsecs. In extreme cases, shock waves may punch through the interstellar medium and form channels for a free gas ejection into the intergalactic space. This last process is known as a galactic superwind.

Such gaseous outflows from starburst regions are important re-distributors of heavy metals, mass, and momentum, and are likely to control the intergalactic medium heating and enrichment by heavy elements during the evolution of the early universe. The outflows are expected to be visible in the X-ray and line emissions.

Indeed, diffuse X-ray emission associated with starburst galaxies has been detected by the *ROSAT*, *ASCA*, *BeppoSAX*, *Chandra*, and *XMM* missions (e.g., Dahlem, Weaver, & Heckman 1998; Pietsch et al. 2000). However, the origin of the soft X-ray emission, the chemical composition of the X-ray emitting gas, and the origin of the broad line ( $\sim 1000 \text{ km s}^{-1}$ ) emission observed in some star-forming regions remain ambiguous (Roy et al. 1992; Strickland & Stevens 1998; Breitschwerdt 2003).

Here, I present numerical solutions for spherically symmetric galactic superwinds, taking into consideration radiative cooling. Two different models, quasi-adiabatic and strongly radiative, are thoroughly discussed, as well as the expected appearance of supergalactic winds in the X-ray and visible line regimes.

### 2. FREE WIND SOLUTION

The prototype galactic superwind model has been proposed by Chevalier & Clegg (1985, hereafter CC85). This model assumes an effective gas thermalization within a star-forming region via collisions of the randomly distributed supernova remnants and stellar winds, as well as free, adiabatic expansion out of the star cluster volume. The legitimacy of this last assumption (the adiabatic condition) has never been carefully analyzed.

Following CC85, I assume a spherically symmetric wind, unaffected by the gravitational pull caused by the galactic dark matter component or an associated central star cluster. I do, however, take into consideration gas cooling out of the star-forming region. The gas dynamic equations then take the form:

$$\frac{1}{r^2} \frac{d}{dr} (\rho u r^2) = 0, \quad (1)$$

$$\rho u \frac{du}{dr} = -\frac{dP}{dr}, \quad (2)$$

$$\frac{1}{r^2} \frac{d}{dr} \left[ \rho u r^2 \left( \frac{u^2}{2} + \frac{\gamma}{\gamma - 1} \frac{P}{\rho} \right) \right] = -Q, \quad (3)$$

where  $r$  is the spherical radius,  $u(r)$ ,  $\rho(r)$ , and  $P(r)$  are the wind velocity, density, and thermal pressure,

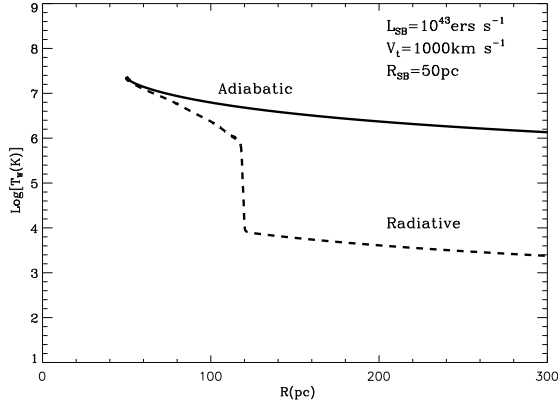


Fig. 1. The intrinsic temperature profiles of the superwind. The solid line represents the adiabatic solution, and the dashed line shows the effects of gas cooling.

respectively. The cooling rate  $Q = n^2\Lambda$ , where  $n$  is the wind number density and  $\Lambda$  is the cooling function.

Three intrinsic parameters control properties of the wind outflow: the mean energy  $L_{SB}$  and mass  $\dot{M}_{SB}$  deposition rates, and the size of the star-forming region  $R_{SB}$ . Note that the total mass and energy deposition rates define the temperature and the sound speed  $c_{SB}$  at the star cluster boundary, which one can then use as an independent parameter instead of the mass deposition rate  $\dot{M}_{SB}$ .

I solve equations (1) to (3) numerically with a realistic cooling function and Solar wind metallicity  $Z_w = Z_\odot$  using the CC85 analytic solution at the star cluster boundary  $R_{SB}$  as the initial condition. It has been found that cooling does not affect the wind velocity nor the density distribution. After crossing  $r = R_{SB}$  the flow is immediately accelerated by the steep pressure gradients and rapidly reaches its terminal velocity ( $V_t \sim 2c_{SB}$ ) and  $r^{-2}$  density distribution. However, the resulting temperature profile is highly dependent on the radius of the star-forming region  $R_{SB}$  and may deviate drastically from the adiabatic value (Figure 1).

One can separate the initial parameter space into the two regions (see Figure 2) by assuming the characteristic cooling time  $\tau_{cool}$  to be equal to the characteristic dynamical time  $\tau_{dyn}$  at some distance  $r$  from the star cluster center. If the initial wind parameters ( $L_{SB}$  and  $R_{SB}$ ) lie below the corresponding terminal velocity curve, cooling is inefficient and deviations from the adiabatic solution are negligible. On the other hand, if the initial wind parameters fall into a region above the corresponding terminal velocity curve, then radiative cooling dominates the wind temperature distribution.

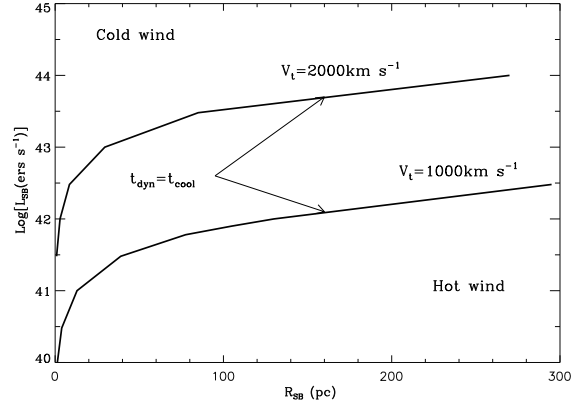


Fig. 2. The separation of the initial parameter space into adiabatic and strongly radiative regions.

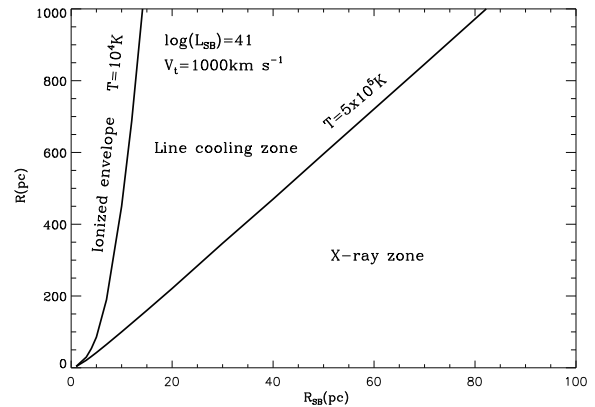


Fig. 3. The internal structure of the free wind outflow.

### 3. COLD WIND OBSERVATIONAL PROPERTIES

Figure 3 represents the structure of the free wind outflow powered by a compact starburst. This includes a star-forming volume, and the adjusting gaseous layers with temperatures higher than the X-ray cutoff temperature  $T = 5 \times 10^5$  K. The intermediate cooling zone has a temperature within the range  $10^4 \leq T \leq 5 \times 10^5$  K. Here, gas cools down effectively and radiates photons additional to those UV photons produced by the stellar content of the cluster. The outer cold envelope has a temperature below  $10^4$  K. This neutral halo is ionized by the UV radiation escaping from the star-forming region and the intermediate zone.

One can easily estimate the ionized zone radius  $R_{st}$  and free wind  $H\alpha$  luminosity from the equation

of ionization equilibrium:

$$\begin{aligned} \frac{dN_{\text{rec}}}{dt} &= 4\pi R_4^2 n(R_4) u(R_4) + 4\pi\beta \int_{R_4}^{\infty} n^2(r) r^2 dr \\ &= \frac{\dot{M}_w}{\mu_a} + \frac{\beta \dot{M}_w^2}{4\pi V_t^2 \mu_a^2 R_4}, \end{aligned} \quad (4)$$

where  $\mu_a = 14/11m_H$  is the mean mass per particle,  $R_4$  is the inner radius of the photoionized zone, and  $\beta = 2.59 \times 10^{-13} \text{ cm}^3 \text{ s}^{-1}$  is the recombination coefficient to all levels but the ground state. The first term in the right-hand side of this equation represents the number of recombinations in the cooling zone and the second one is related to the number of recombinations in the outer cold envelope. The value of H $\alpha$  luminosity is given by the Leitherer & Heckman (1995) relation  $L_{\text{H}\alpha} = 1.36 \times 10^{-12} \dot{N}_{\text{rec}}$ .

Cooling does not affect the general stratification of the free wind outflow (Fig. 3). It does, however, lead to a shrinking of the line radiative zone into a thin layer with a sharp temperature gradient. This effect brings the inner radius of the cold ionized gas envelope and the outer radius of the hot X-ray zone closer to the star cluster center, resulting in a profound impact on the superwind observational properties. The superwind X-ray luminosity falls and becomes more centrally concentrated. Conversely, the H $\alpha$  luminosity becomes larger. This increase is due to denser layers being photoionized when the inner boundary of the cold envelope shifts to the star cluster center.

The difference between adiabatic and radiative model predictions may reach almost two orders of magnitude for a compact star cluster and decreases monotonically with the star cluster size (Figure 4). It is worth noting that cold superwinds form a low-intensity broad ( $\sim 1000 \text{ km s}^{-1}$ ) H $\alpha$  line emission superimposed on a central narrow line component.

#### 4. CONCLUSIONS

Galactic superwinds driven by compact and powerful starbursts undergo catastrophic cooling close to the star cluster surface and establish a temperature distribution radically different to that predicted by the adiabatic model.

The fall of the superwind temperature leads to a smaller zone radiating in X-rays and decreases the superwind X-ray luminosity.

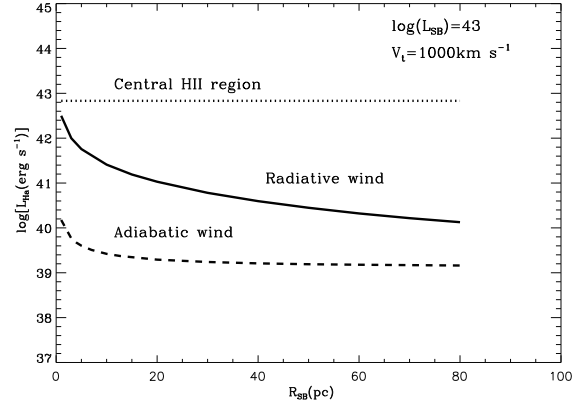


Fig. 4. Superwind H $\alpha$  luminosity as function of  $R_{\text{SB}}$ .

Cooling brings the inner radius of the warm ionized gas envelope closer to the star cluster. This effect increases the estimated H $\alpha$  luminosity and predicts a low-intensity broad ( $\sim 1000 \text{ km s}^{-1}$ ) line emission component.

I am grateful to Guillermo Tenorio-Tagle and Casiana Muñoz-Tuñón for their contributions to the problem discussed in this presentation, as well as José Franco for his friendly remarks and comments. I also thank Edward Chapin for his careful reading of the manuscript. This research has been supported by CONACyT, México grant 36132-E.

#### REFERENCES

- Breitschwerdt, D. 2003, *RevMexAA(SC)*, 15, 311 (this volume)  
 Chevalier, R. A., & Clegg, A. W. 1985, *Nature*, 317, 44  
 Cairo, L. M., Caon, N., Vilches, J. M., González-Pérez, J. N., & Muñoz-Tuñón, C. 2001, *ApJS*, 136, 393  
 Dahlem, M., Weaver, K. A., & Heckman, T. M. 1998, *ApJS*, 118, 401  
 Dawson, S., et al. 2002, *ApJ*, 570, 92  
 Leitherer, C., & Heckman, T. M. 1995, *ApJS*, 96, 9  
 Marlowe, A. T., Heckman, T. M., Wyse, R. F. G., & Schommer, R. 1995, *ApJ*, 438, 563  
 Pettini, M., Kellogg, M., Steidel, C., Dickinson, M., Adelberger, K., & Giavalisco, M. 1998, *ApJ*, 508, 539  
 Pietsch, W., Vogler, A., Klein, U., & Zinnecker, H. 2000, *A&A*, 360, 24  
 Roy, J.-R., Aube, M., McCall, M. L., & Dupour, R. J. 1992, *ApJ*, 386, 498  
 Strickland, D. K., & Stevens, I. R. 1998, *MNRAS*, 297, 747